Original Article

Study of Krypton Laser-Induced Choroidal Neovascularization in a Guinea Pig Model of High Anisometropia

Jianghui Wang[1], Wei Jiang[2], Zefeng Kang[2,*], Lina Liang[2], Xiaoman Liu[2], Nannan Tian[1], Qing Zhang[1]
1 Medical College of Qinghai University, Qinghai 810007, China
2 Eye Hospital of China Academy of Traditional Chinese Medical Sciences, Bejing 100040, China

Abstract

Purpose: To investigate the association between high anisometropia and the area of choroidal neovascularization (CNV) induced by krypton laser in guinea pigs and better understand the pathogenesis and prevention of myopic CNV.

Methods: Nine 3-week old male guinea pigs with anisometropia > 6.00D were randomly assigned to three groups according to examination date after laser photocoagulation (7d, 14d and 28d). All animals underwent refraction. The eye with higher myopia was used as the experimental eye, and the other as the control eye. All eyes received repeated multi-wavelength krypton laser photocoagulation treatments (wavelength: 532 nm; laser power: 400 mW; spot diameter: 50 μm; exposure time: 0.1s). Fundus photography and indocyanine green angiography (ICGA) were performed. Afterwards, the animals were sacrificed immediately, and the eyes were enucleated and processed for histopathologic examination and flat mounts.

Results: CNV appeared at 7d after laser treatment. The area of CNV peaked at 14d, and decrease in area and the presence of scarring was noted at 28 d. CNV was present in 66.7% of eyes by ICGA at 14 d. CNV could be observed under light microscopy at all three time points. At 14 d, flat mount showed the neovascular plexus around the lesion. Semi-quantitative analysis revealed that the area of CNV in treated eyes was greater than that of control eyes.

Conclusion: Since the mechanism of CNV in this study resembles that of CNV in pathological myopia, this model can be used to investigate the etiology, pathogenesis and treatment of CNV in pathological myopia. (***Eye Science 2012; 27: 76–81***)

DOI: 10.3969/j.issn.1000–4432.2012.02.005
Funding: National Natural Science Foundation (grant No. 81072843)
* **Corresponding author**: Zefeng Kang, E-mail: zefeng2531@163.com

Keywords: choroidal neovascularization; high myopia; krypton; laser; animal model

Protein effusion and hemorrhage accompanied by choroidal neovascularization (CNV) are the major reasons for severe loss of vision (e.g., age-related macular degeneration (ARMD)[1–2], pathological myopia, or central exudative chorioretinopathy). However, the pathogenesis of CNV remains elusive, and no effective treatments have been identified[3]. Hence, it is essential to establish suitable CNV animal models to further investigate the underlying pathogenesis and clinical therapy of CNV[4]. The present study, for the first time, analyzes the association between high degree anisometropia and the area of choroidal CNV induced by krypton laser in guinea pigs, and provides pathological evidence for identifying the pathogenesis and prevention of CNV in pathological myopia.

Animals and methods

Animals

Model establishment and grouping: nine 3-week old male guinea pigs (18 eyes) with anisometropia > 6.00D (monocular refraction: −16.00 ~+2.50 D), weighing between 140 and 170 g, were screened from 50 animals by using retinoscopy. The animals used in this study were supplied by Beijing Fangyuanyuan Breeding Factory. Nine animals were randomly divided into three groups 7, 14, and 28d after krypton laser induction (n=3, in each group). The eye with higher myopia was used as the experimental eye, and the other one as normal control. This experiment adhered to the statement of Animals Research in Vision and Ophthalmology.

Experimental equipment: retinoscopy (66 Vision-Tech Co., Ltd, Suzhou, China); A-scan (Biovision, France); multi-wavelength krypton laser (lumenis novas variaXL); Fluorescein fundus angiography and indocyanine green angiography (ICGA) camera (Topcon TRC-501X, Japan); confocal microscope (Olympus IX81, Japan); biomicroscope B204LED (Chongqing Optic Instrument Co., Ltd, China); Image analysis software (Image-Pro Plus 6.0).

Reagents: compound tropicamide eye drops (Santen Pharmaceuticals, Japan); ketamine hydrochloride injection (Fujian Gutian Pharmaceuticals, China); xylazine injection (Jilin Huamu Animal-health Co., Ltd, China); indocyanine green injection (Dandong Yichuang Yaoye Co., Ltd, China).

Methods

Retinoscopy: compound tropicamide eye drops were administered to both eyes of all animals, once per 5 min, 4 times in total. Retinoscopy was performed in a dark room 1h later by two optometrists who were blind to the animals' conditions. The astigmatism was expressed as spherical equivalent. The operating distance was 50 cm, the distance between correct lens and animals' eyes was approximately 5 mm, and the examination was conducted along the direction of optical axis.

Krypton laser photocoagulation: the animals were anesthetized via intramuscular injection of mixed solution of ketamine hydrochloride (35mg/kg) and xylazine (5 mg/kg). Compound tropicamide eye drops were administered for mydriasis, and a 120D super field lens was placed in front of eyes. Krypton laser photocoagulation (wavelength 532 nm) was performed 2 lines above optic disc within one visual field, with 4 spots in each line and 8 points overall. The vapor bubbles were deemed as Bruch's membrane rupture. The spot in which hemorrhage was seen was regarded as invalid spot (laser power: 400 mW, spot diameter: 50 μm, exposure time: 0.1 s).

Fundus examinations and ICGA: the animals in three groups received anesthesia, mydriasis, and fundus examinations before, 7, 14, and 28 d after krypton laser photocoagulation. Indocyanine green was injected into an ear vein of all animals for subsequent ICGA examination.

After ICGA examination, at each time point, one animal was randomly sacrificed, and then the eyes were enucleated, fixed in 4% paraformaldehyde, and transferred in 10% formaldehyde. Under dissecting microscope, cornea, lens, and vitreous body were removed. Neural retinal layer was carefully peeled off. RPE-choroid-sclera was cut 5 to 6 radial incisions, taking optic papilla as symmetry center, placed onto the flat mounts with a slight amount of glycerin gelatin, and sealed for CNV observation under confocal microscope.

Light microscope examination: the remaining two animals in each group were sacrificed at each time point. Then the eyes were enucleated, fixed in 4% paraformaldehyde for 24 h, followed by dehydration in 50%, 70%, and 80% ethanol for 1 h; and in 95% and 100% ethanol for 2 h, and in dimethylbenzene for 15 and 20 min. The specimen was paraffin-embedded and sectioned (5μm in thickness) for H.E staining, and observed under light microscope.

Statistical analysis

SPSS 13.0 software was used for statistical analysis in this study. The data were expressed as $\bar{x} \pm s$. One way ANOVA was used to compare the differences between different groups. Levene's test was adopted to assess the equality of variances in different samples. The CNV areas between experimental and control eyes were analyzed by independent sample *t*-test. $P<0.05$ was considered as a significant difference.

Results

Refraction: All the animals in each group had anisometropia > 6.00D, as shown in Table 1.

Fundus and ICGA examinations: bubbles were observed in the center of 127 out of 144 (88.2%) lasers spots in guinea pigs, and no hemorrhage was noted. If the laser spot destroyed microvessels with bleeding, it was recorded as an invalid spot. The retina-adjacent laser spots became white and presented with acute edema post- photocoagulation. ICGA images revealed that photocoagulation spots presented with fluorescein filling to various extents, confirming that CNV was seen at each time point (Figure 1). The number and percentage of laser pho-

Table 1 Refraction and axial length of both eyes in guinea pigs among three groups (mm)

Eyes	7 d			14 d			28 d		
	1	2	3	1	2	3	1	2	3
R(Diopter)	−10.75	+1.25	+0.50	−4.25	−6.50	−4.75	−8.50	−7.00	−5.00
L(Diopter)	−1.75	−6.00	−13.00	−11.00	+0.125	+2.50	−16.00	−15.50	+1.625
Difference of Refraction	9	7.25	13.5	6.75	6.625	7.25	7.5	8.5	6.625

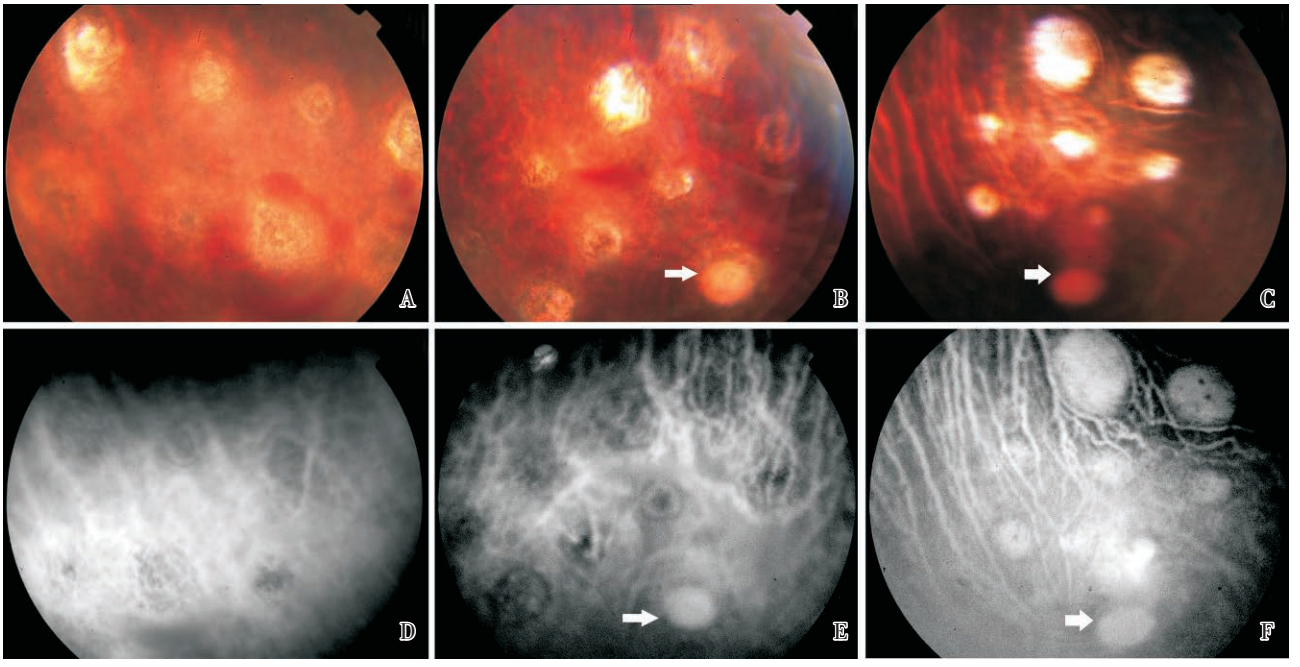

Figure 1 Ocular fundus and ICGA images in the three groups. The ocular fundus images (ABC) and corresponding ICGA images (DEF) at 7, 14, 28 d are depicted respectively. The fluorescence filling in laser spots showed the occurrence of neovascularization. White arrow indicates the optic disk.

tocoagulation spots with fluorescein filling were shown in Table 2.

Table 2 Fluorescence filling spots after photocoagulation with krypton laser among three groups

Time-Point(d)	Effective Spots	Fluorescence filling spots	Percentage
7	44	14	31.8%
14	48	32	66.7%
28	35	21	60.0%

Histopathological examination: healthy guinea pigs had intact retina, choroid, and sclera. Under light microscope, RPE layer and Bruch's membrane rupture were observed at 7 days after laser photocoagulation. Outer nuclear layer defects were seen, and the nuclei of partial inner nuclear layer cells disappeared. Choroidal capillary layer structures were disrupted, and pigment defects were noted. Proliferative cells passed through disruptive Bruch's membrane and RPE via choroid, and migrated towards endoretina, forming early CNV. A variety of cells, including pigment macrophage, neutrophil, migrating, and proliferative RPE and fibroblasts, were seen. Fourteen days after laser photocoagulation, the number of macrophages and neutrophils in CNV decreased. RPE migrated towards interior retina, proliferated, and encompassed CNV. Neovascularization further expanded. At 28 days post-laser photocoagulation, the neovascula continued to grow, the count of pigment macrophage and neutrophil declined, the number of collagenous fiber increased, and neovascula could still be seen (Figure 2).

Choroidal flat mount was used to measure the area of neovascula: fluorescence around laser spots and neovascula was observed at 7 d after laser photocoagulation under confocal microscope; a cluster of

neovascula was seen within and around laser spots, and the vascular area significantly expanded 14 d following laser photocoagulation; 28 d after laser photocoagulation, the area of fluorescence shrank, high-intensity fluorescence was noted in the central laser spots, while peripheral fluorescence disappeared (Figure 3). The area of CNV decreased over time. Image analysis indicated that the respective areas of CNV (μm^2) of the experimental and control eyes in three groups were: 237981.7±20141.2 and 144448.2± 13648.2 (7d); 310859.5 ±25605.0 and 257822.3 ± 37281.8(14d) and; 294472.5±10013.4 and 157851.8± 21300.6 (28d), suggesting that the CNV areas in the experimental eyes were significantly larger than that

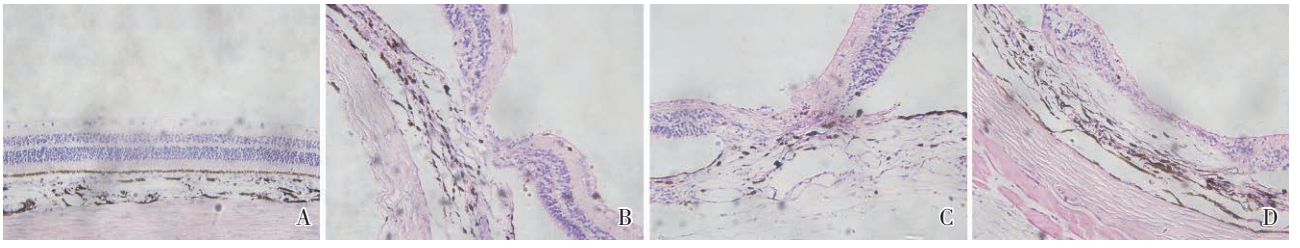

Figure 2 Hematoxylin and eosin staining of choroidal neovascular lesions (× 200). Representative images of normal retina-RPE-choroid (A) and images from lesions on days 7(B),14(C),28(D) after krypton laser photocoagulation are shown.

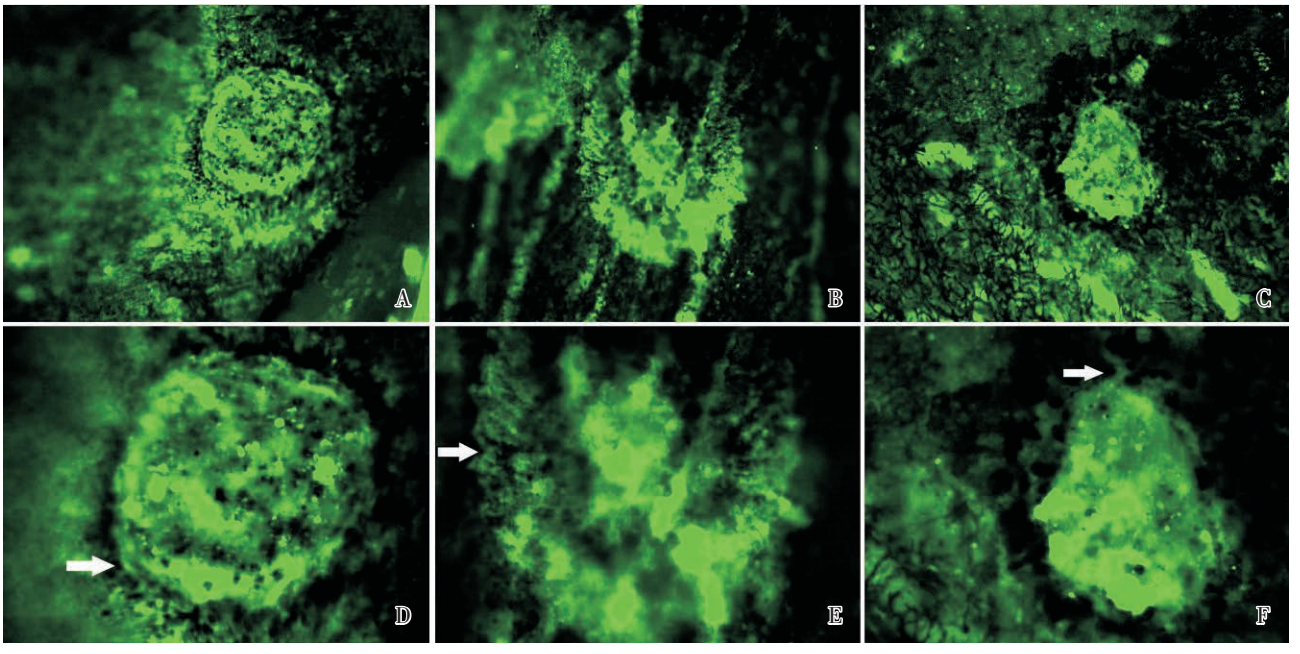

Figure 3 Image of CNV in RPE-choroid-sclera flat mount. The vasculature was labeled with indocyanine (12.5 mg/ml) in guinea pigs after krypton laser photocoagulation. Low (ABC) and high (DEF) magnification representative fluorescent images of laser lesions (arrows) at 7(AD), 14(BE), 28(CF) days respectively.

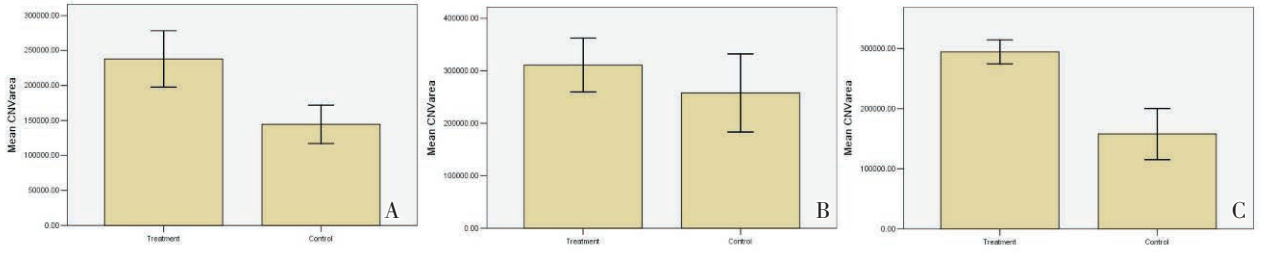

Figure 4 The area of choroidal neovascularization. (A)The area (μm^2)of treatment and control eyes at 7 days. (B) The area of the treatment and control eyes at 14 days. (C) The area of treatment and control eyes at 28 days.

in the control eyes (7 d: t=9.134, P=0.000; 14 d: t=3.023, P=0.012; 28 d: t=10.683, P=0.000). The CNV area post-laser photocoagulation was illustrated in Figure 4.

Discussion

The mechanism of krypton laser-induced CNV in guinea pigs apparently differs from that of human pathological myopic CNV. The former serves to repair laser-induced damages, while for the latter, as most scholars believed, axis oculi extension causes topical tissue traction and rupture, further leading to lacquer cracks (LCs). It is believed that LCs act as a determinant of pathological myopic CNV[6]. Guinea pigs' eyes are characterized as congenital myopic tigroid fundus, and high myopia has been successfully induced by form deprivation[7]. Hence, whether it is feasible or not to utilize krypton laser to induce CNV in guinea pig models with high myopia in an attempt to simulate pathological myopic CNV requires a series of investigations to elucidate. This study is designed to utilize krypton laser to induce CNV in guinea pig models with congenital high-degree anisometropia, and to analyze the association between CNV area and anisometropia.

Laser parameter selection

In this study, multi-wavelength krypton laser (532 nm), high power(400 mW), tiny light spot (50 μm), and short time photocoagulation (exposure time 0.1 s) were collectively adopted to let RPE layer and Bruch's membrane rapidly rupture. CNV formed 7 d after laser photocoagulation; CNV area peaked 14 d post-photocoagulation (model establishment rate 66.7%) and tended to stabilize 28 d following laser photocoagulation. Similarly, Zhao et al[8]. also employed krypton laser (high power 360 mW, light spot diameter 50 μm, exposure time 0.05s) to induce CNV in brown Norway rats, yielding similar results regarding CNV formation. Preliminary results revealed that the laser parameter setup in the present study can successfully induce CNV in guinea pig models.

ICGA evaluation on CNV

Gesine Hubert et al[9]. reported that ICGA can clearly display choroidal vascula of rodent animals. In the present investigation, krypton laser-induced CNV was observed using ICGA because there was no vascula in guinea pigs' retina[10]. The fluorescence filling around the edge of the laser spot was relatively little, and no longer apparent at 7 d post-laser photocoagulation. Significant fluorescence filling noted in laser spot, and the fluorescence filling surrounding the periphery of laser spot increased 14 d after laser treatment. The fluorescence filling 28 d after photocoagulation laser resembled that 14 d post-laser treatment. These results were consistent with corresponding pathological findings.

Histological observations

Similar to laser-induced CNV in alternative rodent animal models[8,11]. Krypton-laser could induce CNV in guinea pigs. Krypton laser mainly produced three types of biological effects, including heat effect, mechanical damages effect, and photochemical effect. Through these effects, laser-induced retinal injuries were able to activate multiple intracellular signaling pathways, entered into tissue repairing phase accompanied by inflammatory reactions. A variety of growth factors and cells got involved in neovascularization. Some scholars proposed a novel idea that CNV formation consisted of two processes: angiogenesis, in which bone marrow-derived cells played a role, and angiogenesis occurring in the form of vessel budding[12].

Seven days after photocoagulation, fibroblasts, vascular endothelia, RPE, etc., were noted in laser spots under light microscope. RPE layer and Bruch's membrane layer rupture was seen in laser spots. Outer nuclear layer was disrupted, and inner nuclear layer was disordered. Proliferative cells passed through disruptive Bruch's membrane and RPE via choroid, and then migrated towards endoretina. Some inflammatory factors, such as pigment macrophage and neutrophil, were found, suggesting that inflammatory cells participated in the formation of CNV. On 14 d after laser photocoagulation, RPE proliferated and migrated towards the interior retina under light microscope, indicating that choroid-derived neovascularization rapidly grew, and vascular cavity was enlarged. Twenty-eight days post-photocoagulation, the amount of pigment macrophage and neutrophil at laser spots declined, while the number of collagenous fibers increased, suggesting that scar ring repairing process was initiated. These results re-

vealed that CNV began to form at 7 d after photocoagulation, peaked at 14 d, and steadily stabilized at 28 d, which were consistent with ICGA findings.

Choroidal flat mount

This study is designed to validate the feasibility of applying krypton laser to induce CNV in guinea pig models. Choroidal flat mount conducted semi-qualitative analysis by using fluorescence intensity, clearly displayed the whole retina, observed and measured the area of laser spots with high resolution, and directly showed CNV. ICGA examination revealed that fluorescence was seen around laser spot, and that neovascularization occurred at 7 d after laser photocoagulation. Fourteen days post-laser treatment, new vessels emerged in cluster peripheral laser spots. A substantial amount of fluorescence was noted in the center and periphery of laser spots, suggesting that the area and intensity of neovascularization further increased. At 28 d after photocoagulation, the size of fluorescence was reduced, high-intensity fluorescence was seen in the central laser spots, and the fluorescence around the laser spots disappeared, indicating that laser spot scarring had begun to form and tissue repairing was initiated.

The results between choroidal flat mount and ICGA examination were consistent, suggesting that the animal models were successfully established in this study. The variation in CNV area at three different time points also confirmed that the CNV began to form at 7 d, CNV area maximized at 14 d, and tended to stabilize at 28 d, and scarring repairing was initiated. Besides, comparing the CNV areas in experimental and control eyes reflected that the CNV area in the experimental eyes with high diopter was larger than that in the controls ones with low diopter. The guinea pigs chosen in the present study resembled human pathological myopia regarding pathological changes, including anisometropia > 6.00D, RPE and choroidal membrane atrophy, LCs formation, etc[13]. Based upon these pathological changes, we assumed that the wall of eyeball was thinned due to high diopter and extended axial length, which led to ischemia and anoxia in choroidal vascula, and eventually caused choroidal and retinal membranes' atrophy. In particular, the posterior wall became thinner, and the area of retinal and choroidal ischemia and anoxia was enlarged. The organism may counteract these adverse factors by neovascularization to nourish choroid and retina.

This study confirmed the feasibility of utilizing krypton to induce CNV formation in guinea pig models using ICGA, histological observation, and choroidal flat mount. In addition, it indicated that the CNV area in the experimental eyes with high diopter was larger compared with that in the control eyes with low diopter. These combined results provide fundamental evidence for subsequently analyzing the pathogenesis underlying pathological CNV. However, the animals with high degree anisometropia can be screened by a larger number of retinoscopy. Therefore, this study has limited sample size, and whether the outcomes deserving wide application requires subsequent investigations to elucidate.

References

1 D′amico DJ. Diseases of the retina.N Engl J Med,1994;331(2):95–106.

2 Lee P,Wang CC,Adamis AP.Ocular neovascularization: an epidemiologic review.Surv Ophthalmologe,1998;43(3):245–269.

3 Yang XM,Wang YS.Animal model of choroidal neovascularization.International Review of Ophthalmology, 2006;30(3):166–170.

4 Bora NS,Kaliappan S,Jha P,et al.CD59,a complement regulatory protein, controls choroidal neovascularization in a mouse model of wet-type age-related macular degeneration.The Journal of lmmunoIogy,2007;178 (3): 1783–1790.

5 Lu F,Zhou X,Zhao H,et al.Axial myopia induced by a monocularly-deprived facemask in guinea pigs: A non-invasive and effective model.Experimental Eye Research, 2006;82(4):628–636.

6 Ikuno Y,Sayanagi K,Soga K,et al.Lacquer crack formation and choroidal neovascularization in pathologic myopia.Retina,2008;28(8):1124–1131.

7 Yang B,Liu GX. Biology and the sclera morphology changes in short-term guinea pig form deprivation myopia model. International Journal of Ophthalmology, 2009;10:1871–1875.

8 Zhao SH,He SZ.Study on the experimental model of krypton laser-induced choroidal neovascularization in the rats.Chinese Journal of Ophthalmology,2003;5:298 – 302.

9 Huber G,Heynen S,Imsand C,et al.Novel rodent models for macular research.

(conti to page 84)